International Journal of
INTELLIGENT SYSTEMS AND APPLICATIONS IN ENGINEERING
ISSN:2147-6799 www.ijisae.org Original Research Paper

Adaptive Neuro-Fuzzy Inference Systembased Bidirectional Battery Charger for Electric Vehicles with Vehicle-to-Grid and grid-to-Vehicle Integration Capability

Mudassirhussain Mahammad, Chandramouli Bethi

Submitted:01/08/2024 **Revised:**20/09/2024 **Accepted:**28/09/2024

Abstract: The giving a free hand for the implementation of the new solution draws on the recently developed rapidity of V2G and G2V technologies for environmentally sustainable transportation. This work describes a bidirectional charger for EV batteries with power management enhancement designed through Adaptive Neuro-Fuzzy Inference System (ANFIS) technology. Technology that permits two-way energy flow enhances EVs' capacity to stabilize the power grid by transforming them into a mobile energy storage unit. The ANFIS-based controller optimizes charging and discharging cycles by modifying control parameters in respect to grid conditions, EV battery state, and power demands. The system has been simulated under various load conditions in MATLAB/Simulink 2021a. The results revealed that this system can stabilize voltage and current waveforms in the grid, maintain state of charge smoothness, improve energy efficiency, and minimize harmonic distortion. The advantages of the ANFIS controller over its conventional counterparts lie in the reduced computational burden and the possibility of real-time decision support. These results substantiate the proposition that V2G technology coupled with smart control systems can contribute immensely to energy efficiency, peak load reduction, and grid stabilization. Suggested future efforts will involve real-time hardware implementation, improvement of AI optimization devices, and integration with renewable sources, thereby boosting the efficiency and scalability of the proposed system.

Keywords: *Vehicle-to-Grid (V2G), Grid-to-Vehicle (G2V), Bi-directional battery charger, Adaptive Neuro-Fuzzy Inference System (ANFIS), Electric Vehicle charging, Power Grid Integration.*

1 Introduction

Rising oil prices, increasing energy demand, and climate change underscore the urgent need to shift away from hydrocarbon-based transportation[1]. Fossil fuel-powered transport contributes around 16% of global CO_2 emissions, negatively impacting air quality and public health. Plug-in Electric Vehicles (PEVs), with their higher efficiency and lower operating costs compared to Internal Combustion Engine (ICE) vehicles, are expected to see a surge in adoption [2]. However, the widespread use of PEVs raises concerns about grid reliability, especially at the low-voltage distribution level. Despite their benefits, adoption faces challenges such as high costs, limited battery life, charging infrastructure gaps, long travel ranges, and power quality issues like line losses and harmonics [3].

Research scholar, Department of EEE , Chaitanya deemed to be university, Himayathnagar , Moinabad, Hyderabad-500075.

Professor , Department of EEE, Chaitanya deemed to be university, Himayathnagar, Moinabad, Hyderabad-500075.

Smart grids aim to integrate distributed energy resources, storage systems, and PEVs to enable the use of renewable energy at scale. Yet, the intermittent nature of renewables complicates grid control. Utilities must address issues like peak load reduction, reactive power compensation, and maintaining power quality [4]. PEVs with Vehicle-to-Grid (V2G) capabilities can help by acting as "prosumers," supporting the grid with services like load balancing and frequency control through their onboard energy storage systems (ESS) [5]. To achieve this, fast charging stations must mitigate power quality issues and improve power factor. However, charging large numbers of electric vehicles (EVs) simultaneously may lead to high Total Harmonic Distortion (THD), voltage instability, and frequency disturbances. These problems can be alleviated through grid upgrades or integrating renewable sources like solar and wind although their variability necessitates reliable energy storage solutions.

Simultaneously, electrical systems are presently encountering many obstacles: To start, energy consumption is on the rise due to the digitalization of the world [6]. Secondly, power network supply-

and-demand equilibrium is made more complicated by the addition of intermittent renewable energy sources. [7]. Third, problems with grid stability are getting worse as EVs become more common. From 30 million in 2022 to around 240 million in 2030, an increase of eightfold, is predicted by even the most cautious growth estimates for the electric car market. Increased network power storage capacity is necessary to address these challenges [8]. As an example, bidirectional charging allows power to flow both from the grid to the electric vehicle and back, forming a key part of smart grid advancements. Technologies like V2G are central to this digital energy revolution. V2G can further expand into broader concepts such as V2X (Vehicle-to-Everything), including V2V (Vehicle-to-Vehicle), V2B (Vehicle-to-Business), and V2H (Vehicle-to-Home), enabling energy transfer from vehicles to various systems.

As the global energy shift emphasizes renewables and system modernization, EVs are increasingly seen as portable energy assets [9]. V2G integration marks a major paradigm shift by enabling two-way energy flow between EVs and the grid, enhancing grid stability and resilience [10]. Figure 1 presents a simplified V2G ecosystem that includes EVs, renewable energy sources such as solar and wind, energy storage systems, and bidirectional chargers. It highlights key functions like frequency regulation, peak shaving, and load balancing enabled by two-way energy exchange. The visual representation uses a minimalist design for clarity. With V2G and smart grid technologies progressing together, there is growing collaboration among researchers, industry, and policymakers to address the technical, commercial, and legal dimensions of V2G systems [11]. While innovative studies have showcased the utility of EV batteries for grid services, gaps remainparticularly regarding regulatory frameworks and economic feasibilitythat must be addressed for successful large-scale V2G adoption [12].

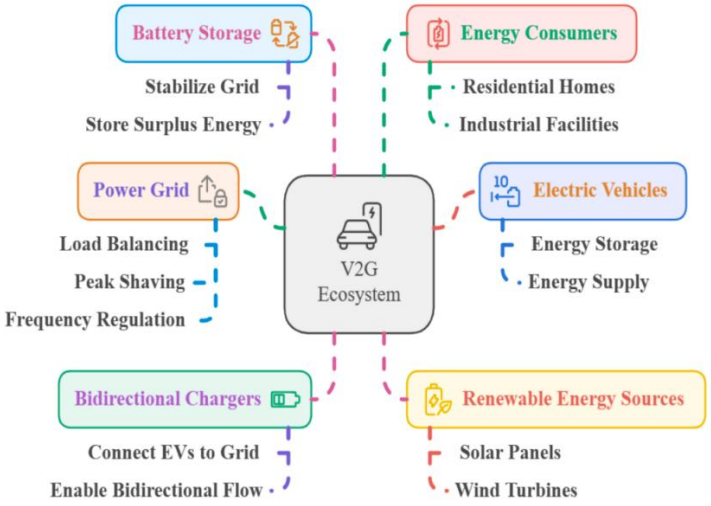

Figure 1 V2G Ecosystem

Bidirectional power flow enables EVsto both draw power from the grid and supply it back using Vehicle-to-Grid (V2G) networks. This is facilitated through bidirectional Electric Vehicle Supply Equipment (EVSEs), allowing EVs to function as energy storage units that support grid services like load balancing and frequency regulation [13]. Unlike conventional chargers, bidirectional systems allow simultaneous charging and discharging, helping reduce peak grid demand and enhancing grid stability [14]. EV owners also benefit economically by charging during off-peak hours and selling excess energy back to the grid, thus lowering overall ownership costs [15]. Recent innovations in power electronics and charge management have enabled real-time communication between chargers and the grid, improving energy transfer efficiency. While Grid-to-Vehicle (G2V) charging is cost-effective and reduces battery wear, V2G provides additional grid support and financial incentives, albeit with potential battery degradation due to frequent charge-discharge cycles.

The rapid growth of PEVs presents both opportunities and challenges for modern power systems. While PEVs are environmentally friendlier than internal combustion engines, their

impact on peak loads, power quality, and battery life due to grid integration is concerning. Traditional V2G systems struggle with real-time demand variability, limited adaptability, and inefficient control strategies, leading to battery strain and energy inefficiency. To address this, the study proposes an intelligent control framework using Fuzzy Logic and Adaptive Neuro-Fuzzy Inference System (ANFIS). This system enables real-time, bidirectional charging by aligning energy exchange with grid status, battery condition, and renewable energy availability. By leveraging ANFIS's learning ability and fuzzy logic's decision-making, the framework enhances grid stability, improves energy efficiency, reduces harmonic distortion, and minimizes battery degradationadvancing smart, sustainable V2G integration.

2 Related Work

Problems arise for power systems due to the rising demand for energy caused by digitalization, renewable energy, and electric cars. V2G technology offers cost-effective energy storage solutions. [16] explored stakeholder roles, potentials, and challenges in V2G architecture, focusing on consumer, V2G systems, power markets, and communication operators. It highlights the importance of data collection, utilization, and sharing in a bidirectional charging environment. [17] examined advancements in electric vehicle battery technology, charging protocols, and the use of artificial intelligence to improving electric vehicle performance. Because of their low price, Due to their long lifespan, great energy density, and dominance in the industry, lithium-ion batteries. However, these batteries are quite sensitive to changes in temperature. The potential solution for increased energy density and faster charging is solid-state batteries, even if they face a number of challenges. The study indicated that policy and technology advancements must tackle battery recycling, material shortages, and charging infrastructure. [18] presented a bidirectional charger circuit for electric two/three wheelers, achieving high voltage step-down, controlled ripple content, and low switch count. The charger made use of a voltage source converter and an adjusted single-ended primary-inductance converter (SEPIC). The circuit's effectiveness is validated through experimental investigation, achieving over 90% efficiency under different conditions. [19] investigated the use of a V2G-enabled bidirectional off-board electric vehicle battery charger for grid current harmonic compensation and reactive power compensation. In order to estimate the active load current components and synchronization voltage templates, the control algorithm makes use of nonlinear residential load current and point of common coupling voltage. Simulation results and an experimental prototype are used to validate the results.

[20]analyzed the role of V2G technology in supporting Spain's 2030 and 2050 energy goals through EV battery-based storage. A validated Simulink model projected that by 2030, EVs could replace 122 GW of storage, with 2.7 TW needed by 2050 for large-scale renewable integration. Importing 18 TWh of electricity and installing 800 GW (or 220 GW) of solar and wind by 2030 could enable 42% renewable energy, while 50 TWh imports by 2050 could achieve 97% green energy. V2G helps reduce storage infrastructure needs and enhances grid stability. [21] highlighted challenges in meeting round-the-clock electricity demand amid increasing reliance on variable renewable energy and electrification. Flexibility in generation and demand, supported by sector coupling, storage, and grid upgrades, is crucial. The LUT Energy System Transition Model shows that smart charging and V2G can reduce storage needs, capacity, and system costs, even with high operational costs. [22]noted that while smart charging partially reduces EV-induced peak demand, it only lowers the increase from 36–51% to 30–41% across Europe. [23] emphasized that the global impact of fossil fuels is driving efforts toward carbon-free, energy-efficient transportation. EVs offer a solution, but scaling electricity generation and infrastructure remains a challenge. V2G, though still emerging, offers economic and environmental benefits by linking EVs with the grid. [24] further discussed how the rapid growth of EVs opens up opportunities to adopt clean energy in transport. The affordability and simplicity of on-board chargers (OBCs) have led to widespread use, and bidirectional power flow solutions are gaining popularity. The study provided insights into current technologies, promising topologies, and future trends in this area.

2.1 Research Gap

While significant progress has been made in smart charging, grid stability, V2G technologies, and bidirectional charger designs, several barriers still hinder large-scale adoption. Key challenges include the absence of legislative incentives, regulatory frameworks, and standardized business models. Most existing studies emphasize grid efficiency, with limited focus on the long-term effects of bidirectional charging on battery health and user behavior. Additionally, the integration of V2G with renewable energy sources and optimization of energy flows to reduce grid dependency remains underexplored. The lack of V2G-ready electric vehicles further highlights the market's unpreparedness. A comprehensive approach combining technological, economic, and regulatory advancements is needed to enable effective V2G integration.

3 Background

3.1 Power Electronic Charging Topology

Efficient and cost-effective manufacturing of battery chargers remains a key challenge to the widespread adoption of EVs, as charger performance directly impacts battery life, charging time, and overall efficiency [25]. Designing chargers with high efficiency, low cost, minimal power losses, and strong power factor correction is essential [26]. With the growing number of EV charging stations, optimizing the grid interface with Plug-in Electric Vehicles (PEVs) requires advanced chargers and management systems. Power Electronic Converters (PECs) are crucial in linking EVs, energy storage systems, and renewable energy sources (RESs) [27]. Numerous studies have reviewed PEC classifications, configurations, control strategies, applications, and their impact on grid power quality [28]. Common PEC architectures in EVs include various charger setups and DC-DC converters, with topologies such as DC-DC, AC-DC, DC-AC, and AC-AC used for both low- and high-voltage applications.

The ideal charger features bidirectional power flow (V2G and G2V), unity power factor, effective power management, minimal power quality impact, simple design, and compatibility with a standard 16 A single-phase plug . With a 2.3 kW output, it suits household use, adhering to EU standards and grid limits. As shown in Figure 2, the charger uses insulated gate bipolar transistors (IGBTs) for efficient, high-speed switching. The AC/DC converter rectifies voltage in G2V mode and inverts it in V2G mode. LC filters aid in energy storage and noise reduction, while buck and boost modes handle power flow in each operation mode.

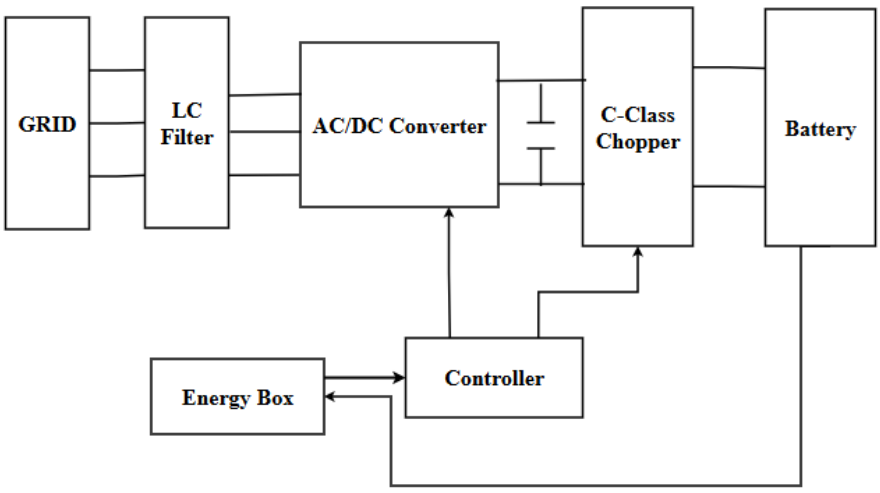

Figure 2 : PEV charger topology

3.2 DC/DC Converter Circuit Analysis

Bidirectional DC-DC converters (BDCs) can reverse power flow in response to control commands, enabling DC voltage conversion in both directions. In vehicle-to-grid systems, BDCs serve dual roles: adjusting voltage for charging in G2V mode and matching DC side voltage in V2G

mode [29]. They typically operate in two stages—constant voltage and constant currentto efficiently charge EV batteries. High switching frequencies in BDCs boost power density but can generate electromagnetic interference (EMI), affecting other grid-connected devices. Hence, effective EMI reduction and control are essential in BDC design.The DC/DC converter can operate in the first two quadrants, including positive voltage and both negative and positive current circumstances, thanks to class C hopping. For buck mode, the principal operational equations may be expressed as (1) through (4), and for boost mode, as (5) through (8).

$$V_{BAT} = V_{Cbus} - L_{Chopper}.\frac{dI_L}{dt} \quad (1)$$

$$I_L = \frac{1}{L_{Chopper}}.\int_0^{T_{on}}(V_{Cbus} - V_{BAT})\,dt \quad (2)$$

$$V_{BAT} = -L_{Chopper}.\frac{dI_L}{dt} \quad (3)$$

$$I_L = \int_{T_{on}}^{T_{off}} \frac{V_{BAT}}{L_{Chopper}} dt \quad (4)$$

$$V_{BAT} = L_{Chopper}.\frac{dI_L}{dt} \quad (5)$$

$$I_L = \frac{1}{L_{Chopper}}.\int_0^{T_{on}} V_{BAT} dt \quad (6)$$

$$V_{BAT} + V_{LChopper} = V_{Cbus} \quad (7)$$

$$I_L = \frac{1}{L_{Chopper}}.\int_{T_{on}}^{T_{off}}(V_{BAT} - V_{Cbus})\,dt \quad (8)$$

The ratio relationship between the helicopter sides may be managed with the use of Pulse Width Modulation (PWM) signals; each power switch has a single switching period (T) that includes the driving duration (Ton) and cut-off time (Toff). Regarding the buck mode, the duty cycle (D) is defined by equations (9) and (10) and for the boost mode, by equations (11) and (12). This duty cycle determines the voltage conversion ratio of the circuit [26].

$$D = \frac{T_{on}}{T} \quad (9)$$

$$V_{BAT} = V_{Cbus}.\frac{T_{on}}{T} = V_{Cbus}.D \quad (10)$$

$$\frac{1}{1-D} = \frac{V_{Cbus}}{V_{BAT}} \Leftrightarrow D = -\frac{V_{BAT}}{V_{Cbus}} + 1 \quad (11)$$

$$V_{BAT} = V_{Cbus}.(1 - D) \quad (12)$$

The inductor ($L_{Chopper}$) and the DC bus capacitor (C_{bus}) essential to the operation of this converter. In either boost or buck mode, the inductor determines how much energy needs to be released on each side of the helicopter. In addition to reducing the impact of high switching frequencies, it aids in controlling source current ripple [26]. Regardless of the mode of operation, the inductor's size is determined by the increased power output with a drop in battery voltage. Equation (14)'s output in buck mode is:

$$L_{Chopper} = \frac{V_{Cbus} - V_{BAT}}{2.\Delta I_L} \quad (13)$$

$$DT = T_{on} \rightarrow \begin{cases} T_{on}\_\min = & \frac{V_{BAT_{\min}}}{V_{Cbus}}.T \\ T_{on}\_\max = & \frac{V_{BAT_{\max}}}{V_{Cbus}}.T \end{cases} \quad (14)$$

3.3 AC/DC Converter Circuit Analysis

The proposed charger uses an AC/DC converter that functions as a rectifier during charging (AC to DC) and as an inverter during discharging (DC to AC) for grid support. It achieves reduced voltage ripple and improved efficiency using a unipolar PWM technique and low-resistance IGBT. The PWM controller sends gate pulses and controls the converter's operating mode.

4 Controllers Design

The ANFIS-based controllers' stated goal is to regulate the switching of the IGBT in accordance with the specified voltage and current.

4.1 Chopper Controller

You can see the controller design for the helicopter in Figure 3 down below. G2V and V2G are the two operating modes that were put into place. Two currents, one for G2V and one for V2G, will be computed by this controller. The measured Vbus voltage is contrasted with the actual Vbus voltage in both cases. Next, the voltage PI controller receives the error signal, together with the current and voltage inputs from the battery [30]. For both G2V and V2G actions, this ANFIS controller generates current as an output. In order for the G2V operation to be carried out, the energy box's power must be greater than zero. The V2G function is activated when the power of the energy box is negative. The ANFIS controller receives the current signal and converts it to a voltage signal. The pulse width modulator (PWM) generator receives this voltage signal and uses it to generate gate pulses for the helicopter. These pulses determine whether the DC-DC converter is a buck or a boost converter.

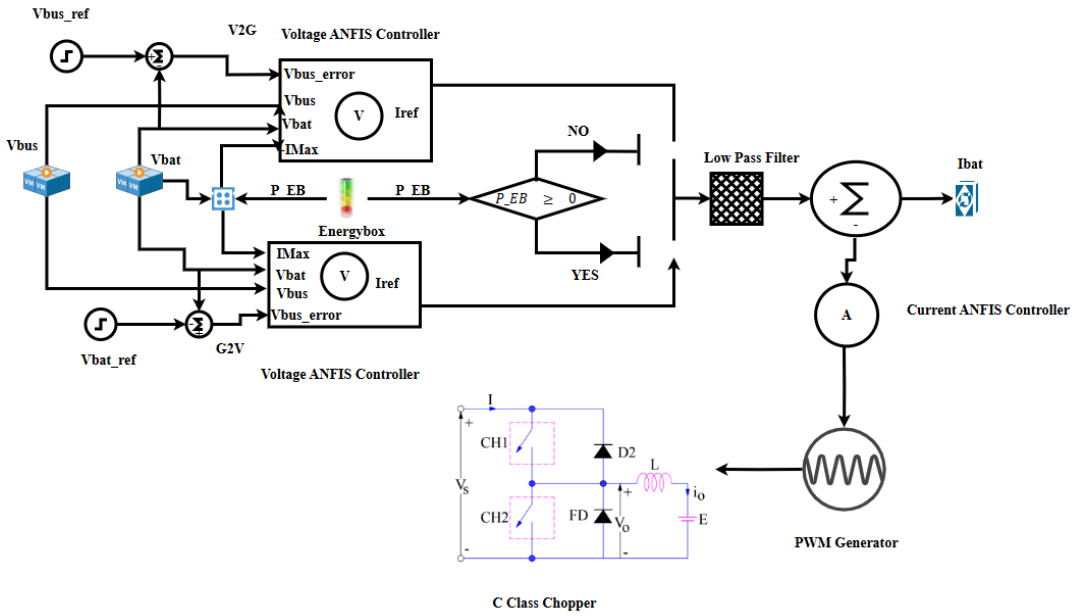

Figure 3 DC/DC converter controller architecture for V2G and G2V operation modes, respectively

4.2 Fuzzy Logic Controller

Because of its versatility and ability to handle nonlinearities and uncertainties, Fuzzy Logic Controllers (FLCs) have found extensive usage in power electronics. FLCsmake decisions based on fuzzy input data using a set of language rules and membership functions. In cases where the system dynamics are complex and not amenable to accurate modeling, this technique becomes invaluable. The main advantages of FLCs are robustness, range of applicability, easy design, and implementation [31].

FLCs are crucial in EV battery charging systems for optimizing charging, enhancing power quality, and maintaining system stability. They effectively manage bidirectional energy flow and reduce battery aging, and their flexibility allows integration with control methods like Model Predictive Control (MPC) and Proportional-Derivative-Integral (PDI) controllers.The FLC design involves key steps: selecting input variables such as grid power demand, battery State of Charge (SOC), and State of Health (SOH); defining fuzzy sets and membership functions; creating expert-based fuzzy rules; designing an inference engine to determine control actions; and using defuzzification to generate accurate real-time control signals (Figure.4).

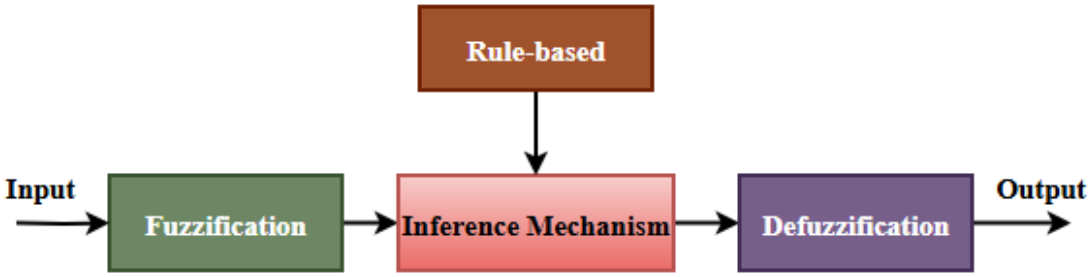

Figure 4 Fuzzy logic controller block diagram

4.3 An Adaptive neuro-fuzzy inference system (ANFIS)

ANFIS is a network that mimics the behavior of FIS and neural networks. While both adaptive and non-adaptive nodes are provided by the adaptive neural network, synaptic weights are not. By transforming it from its most well-known forma traditional architecture of feed-forward neural networksan adaptable network will be built [32]. An adaptive Takagi-Sugeno fuzzy controller emulator has an ANFIS adaptive network-like design. This adaptive network works like a Flexible Interface (FI). Back-propagating, the ANFIS network employs gradient descent and least squares to select input and output parameters for the input/output data set. The ANFIS network's input and output parameters characterize its linear and nonlinear behavior. The predecessor and successor components of ANFIS are crucial. Each portion is connected by a rule-based structure and FIS.The overall architecture is shown in Figure 5, illustrating the five-layer ANFIS structure and the flow of data and decision-making across the network.

The fundamental principle of ANFIS, with two inputs x1 and x2, and a single output y, may be articulated as follows.

- Rule 1: if x_1 is A_1 and x_2 is B_1, then $y_1=p_1x_1+q_1x_2+r_1$
- Rule 2: if x_1 is A_2 and x_2 is B_2, then $y_2=p_2x_1+q_2x_2+r_2$

The fuzzy set parameters for each input in part-if (permissive portion) are Ai and Bi, while the linear parameters in part then are Pi, qi, and ri(consequent peart).

Layer 1:

An adaptive node, Node I in this layer is what makes up the ANFIS network's nonlinear parameters. Each node's role is, according to Equation (16),

$$L_{1,I} = \mu A_i(e) \quad (15)$$

$$L_{1,I} = \mu B_i(\Delta e) \quad (16)$$

In layer 1, the inputs of node i are represented by e and Δe. Ai and Bi are the membership functions for every node. A Gaussian membership function is commonly used to disperse the input variables; this function assigns a membership function to each node in the network. Consequently, Equation (17) delineates the function of Gaussian membership as follows.

$$f(x;\sigma,c) = \frac{-(x-c)^2}{2\sigma^2} \quad (17)$$

In the context of the Gaussian membership function, σ represents its breadth and c stands for its center. Nonlinear characteristics that change throughout learning are the width and center parameters.

Layer 2:

The signal for a static output node, represented by the symbol " Γ ", is obtained by multiplying the signals of the nodes in Layer 1 together. Eq. 18 represents the node function.

$$L_{I,K} = W_i = \mu A_i(e)\mu B_i(\Delta e) \quad (18)$$

The output of each layer 2 node dictates the firing strength of the rule basis.

Layer 3:

"N" stands for the "layer node," sometimes called a fixed node. To get the result, we take the total node value and divide it by the value of each node. An equation describing the node function is given by (19).

$$L_{3,I} = W_i = \frac{w_i}{\sum_i^{j^2} w_i} \quad (19)$$

Layer 4:

This node is versatile. The operation of this node is articulated as shown in Equation (20).

$$L_{4,I} = \overline{W_l}\, f_i = \overline{W_l}(p_i e + q_i \Delta e + r_i) \qquad (20)$$

The ANFIS network's linear parameters, sometimes called network consequent parameters, and the normalized layer 3 firing intensity are located. These parameters are adjusted throughout the learning phase by employing the least squares method.

Layer 5:

The sign "∑" represents a fixed node in the output layer. To determine the output from this layer, we utilize the weighted average approach, as shown in equation (21).

$$L_{5,I} = \sum_{i=1}^{j^2} \overline{W_l}\, f_i \qquad (21)$$

Layers 2 and 4 were updated using a hybrid ANFIS method that combines least-squares for tuning linear parameters during forward propagation and gradient descent for adjusting nonlinear parameters during backward propagation. This bidirectional approach accelerates convergence by reducing search dimensions compared to standard backpropagation techniques.

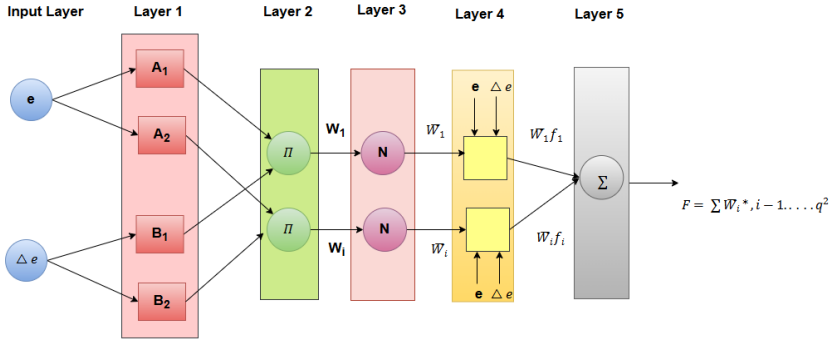

Figure 5 Five Layer ANFIS Structure

5 Results

The simulation is carried out in MATLAB Simulink in 2021. Table 1 and Figure 6 depict the system architecture and its simulation parameters. Figure 6 shows the plug-in electric vehicle's connection to the utility through the wall charger box, which houses the battery switching control, AC-DC converters, DC-DC converters with battery controllers, and DC-AC/DC converters with buck-boost, all of which are available. As mentioned in the approach section, an improved ANFIS algorithm-based model reference adaptive controller accomplishes the battery controller's control action. A model reference adoption controller is part of the intended control unit for the battery charger, as shown in Figure 7.

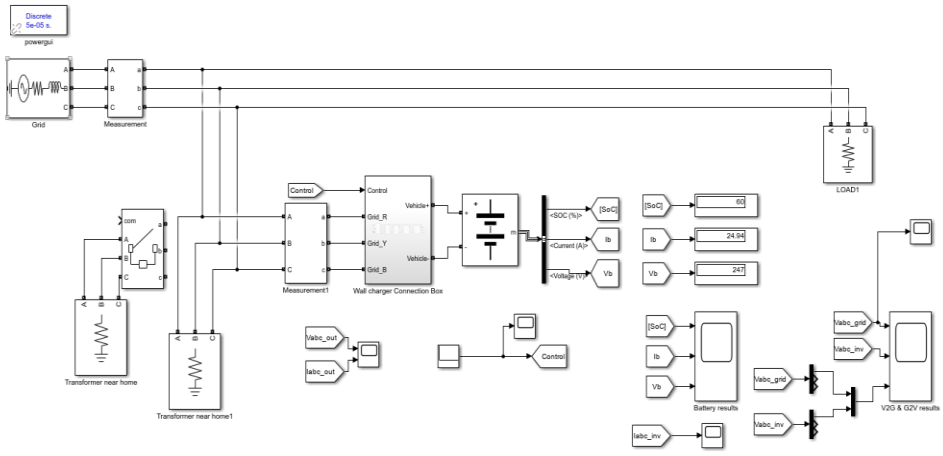

Figure 6 Design System Architecture

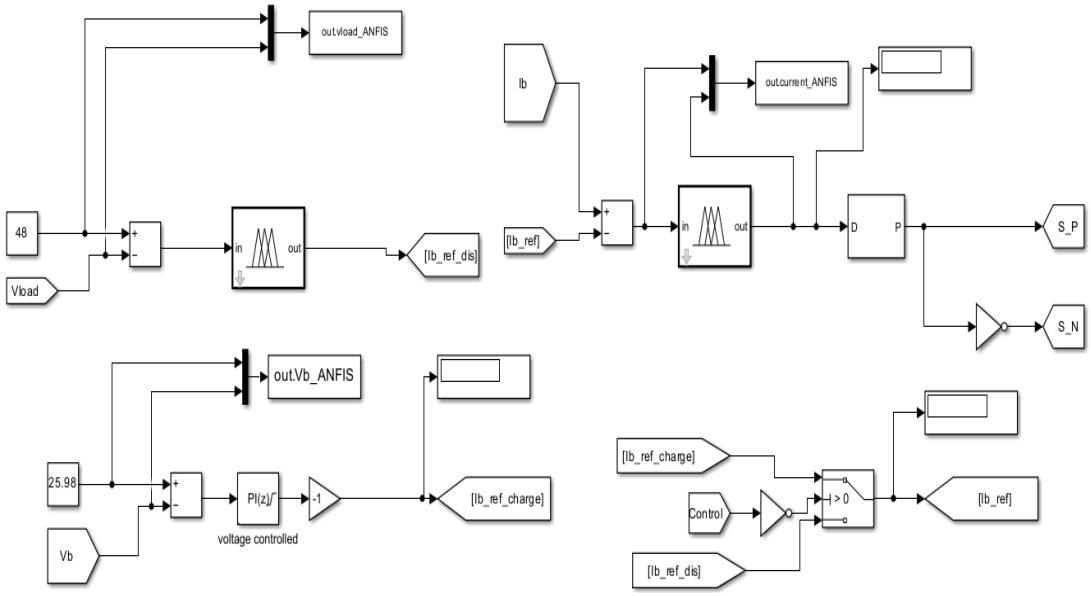

Figure 7 System design of ANFIS Controller

Table 1 Specifications and parameters of the system

Network Components	**Parameter Values**
Load	Active Power(P): 1KW Nominal Phase-to Phase Voltage (Vn) = 380 V
Transformer	Delta (D1), Yg (Wye-grounded) 11 KV/ 0.4V, 20 KV/173 V R1=R2=0.003 p.u, L1=L2=0.08 p.u.
Source	V_{L-L}=20kV, f=60Hz
Nominal frequency (Hz)	50
Active Power P (W)	20e3
Inductive reactive Power QL (positive var)	0
Capacitive reactive Power Qc (negative var)	0

5.1 Vehicle to Grid

In the V2G operation, the system's performance is evaluated through multiple waveform observations that reflect the interaction between the electric vehicle, battery, inverter, and the grid. Figure 8 illustrates the vehicle's output voltage and current over time. The top plot displays three-phase output voltages (Va, Vb, and Vc) in red, blue, and green, each showing a high-frequency sinusoidal waveform characteristic of AC systems. The bottom plot demonstrates the corresponding three-phase output currents (Ia, Ib, and Ic) with square-wave patterns, indicating the application of pulse-width modulation (PWM) control. The system reaches a stable operating condition shortly after the initial transient response, as evident from the waveform behavior within the 0 to 0.5-second time frame.Figure 9 provides insights into the battery's behavior during V2G operation. The top plot shows the SOC of the battery, represented by a steadily rising blue line, indicating active charging or a net energy gain. The center plot displays battery current (in red), which remains relatively stable, suggesting a consistent current flow. The bottom plot shows battery voltage (in green), which remains nearly constant, indicating well-regulated

voltage levels. These waveforms confirm effective control of the battery charging process and system stability.

Figure 10 presents three comparative voltage graphs. The first shows three-phase grid voltages (Va, Vb, and Vc) oscillating symmetrically around zero, validating a steady and balanced AC power source. The second graph shows inverter voltage output, which is consistent, indicating effective regulation. The third plot compares a single-phase voltage from both grid and inverter, revealing high synchronization and alignment between the two, essential for efficient bidirectional energy transfer.Figure 11 presents a single flat line for inverter current over time, remaining at zero, suggesting either an idle or balanced state where no significant variation occurs in current levels. Finally, Figure 12 depicts a clean and consistent three-phase voltage waveform from the grid, with sinusoidal oscillations around ±500V, indicating a stable power supply. Collectively, these figures demonstrate the system's ability to maintain power quality, voltage stability, and synchronization during V2G operations, confirming the efficacy of the proposed intelligent control strategy.

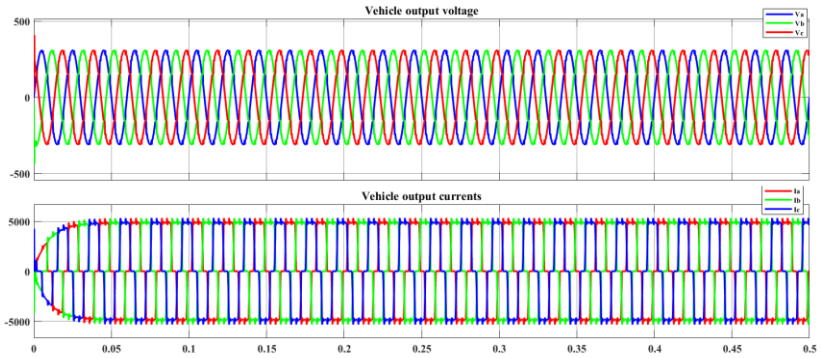

Figure 8 Vehicle Output Voltage and Currents

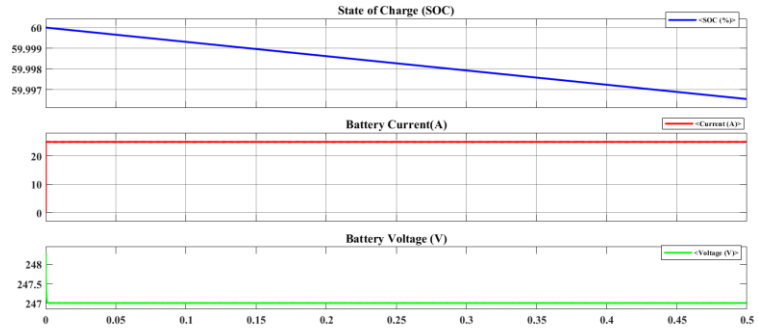

Figure 9 Battery Results

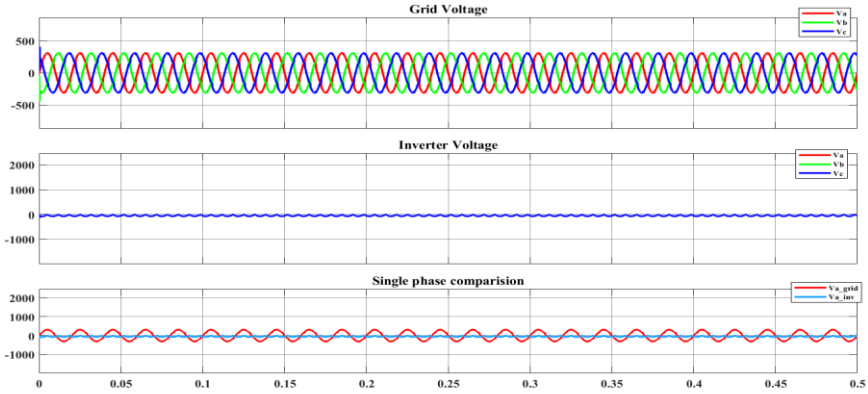

Figure 10V2G & G2V Voltages

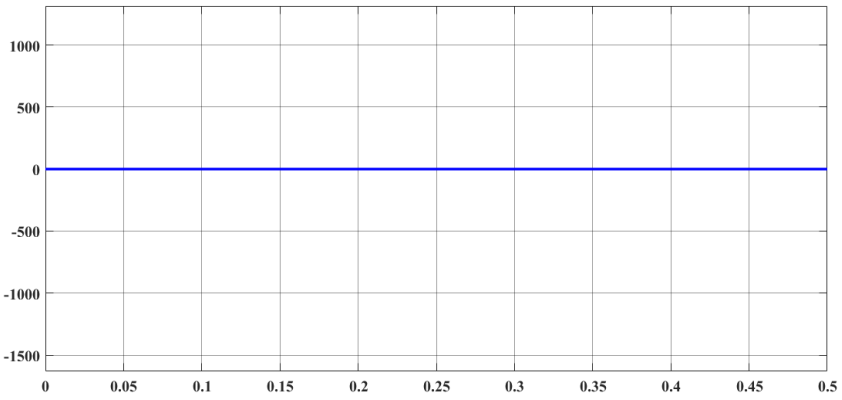

Figure 11 Inverter currents

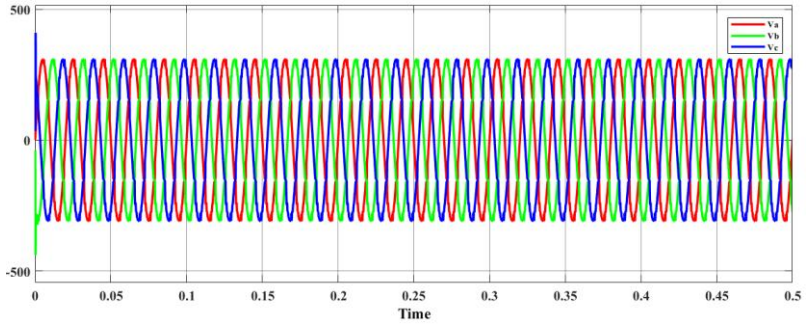

Figure 12 Voltage Grid

5.2 Grid to Vehicle:

Multiple waveform representations that emphasize reliable energy transmission from the grid to the EV are used to assess system performance in G2V operations. A red line in Figure 13's single-plot graph of inverter current continuously maintains a value of around 1 per unit between 0 and 0.5 seconds. A well-balanced and controlled system is implied by this stable, almost flat behavior with no oscillation, which might be a normalized power factor or voltage characteristic. The three-phase output voltage and current waveforms for the vehicle are shown in Figure 14. With amplitudes of around ±500V, the sinusoidal, symmetrical voltage signals (Va, Vb, and Vc), which are shown in red, blue, and green, respectively, verify a steady AC supply. A steady-state operation is reflected by the associated current waveforms (Ia, Ib, and Ic), which at first show a brief response before rapidly settling into low-amplitude oscillations.

Figure 15 focuses on battery performance during charging. As shown in the blue plot at the top, the SOC drops from 60%, signifying discharge in this mode. The green bottom plot displays a fairly constant battery voltage of around 247.5V, while the red mid-plot displays a stable battery current of about 20A. These point to a consistent and easy battery discharge procedure. Grid voltage, inverter voltage, and their single-phase alignment are compared in three panels in Figure 16. The first panel uses sinusoidal three-phase waveforms (Va, Vb, and Vc) to verify grid stability. Excellent synchronization is suggested by the second panel, which displays that the inverter voltage nearly resembles the grid voltage. When single-phase voltages from the grid and inverter are compared in the last panel, there is very little phase and magnitude variation, which is essential for smooth bidirectional power transmission. Three-phase inverter currents (Ia, Ib, and Ic) are shown in red, green, and blue in Figure 17. Due to early transients, these waveforms start off with growing amplitude before stabilizing into balanced sinusoidal forms with a 120° phase shift, demonstrating effective performance at high switching frequencies. The grid voltage waveform over 0.5 seconds is shown in Figure 18. A harmonic-free, balanced, and well-regulated AC supply appropriate for precise applications such as EV charging and renewable power integration is confirmed by the three-phase voltages, which display pure sinusoidal signals with an amplitude of ±300V and a phase shift of 120°.

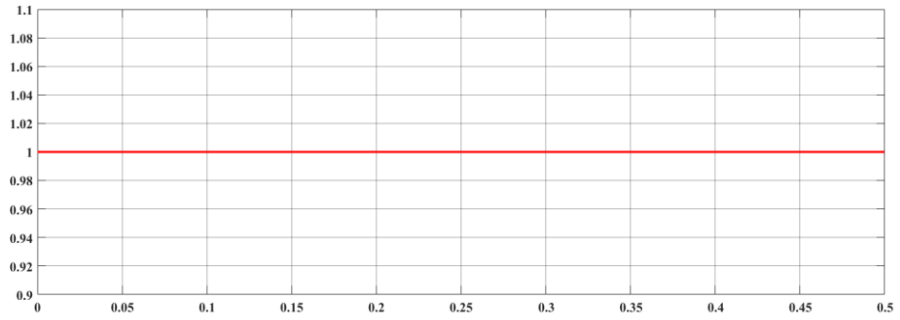

Figure 13 Inverter Currents

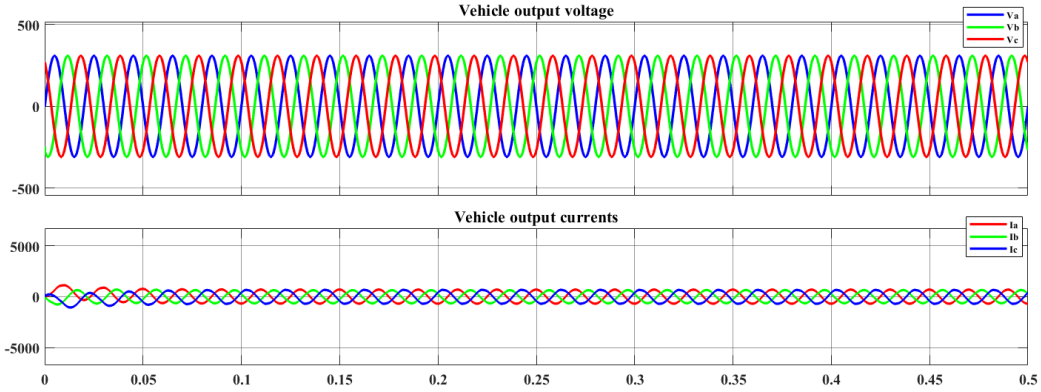

Figure 14Vehicle Output Voltage and Currents

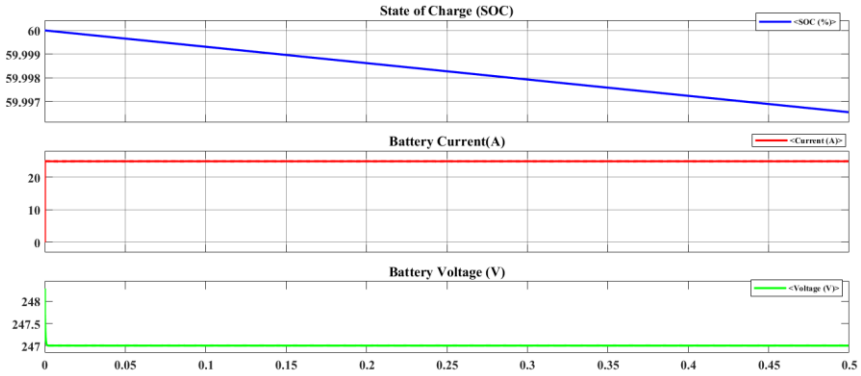

Figure 15 Battery Results

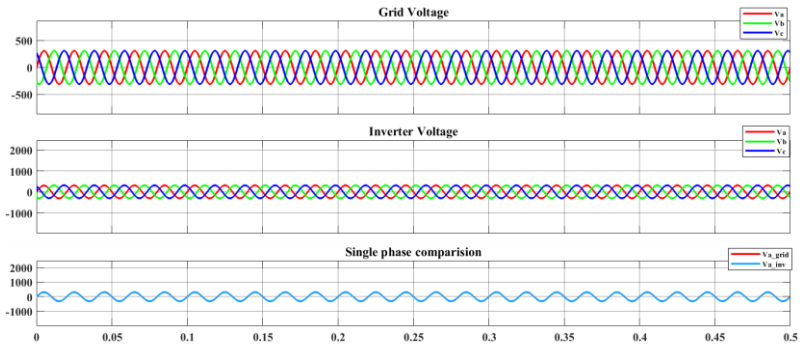

Figure 16 V2G & G2V Results

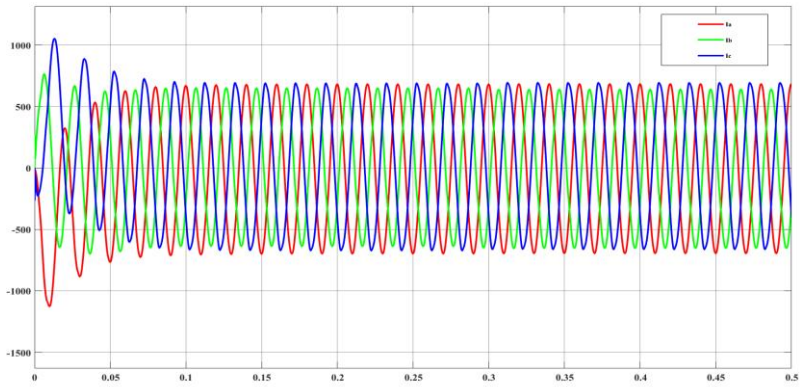

Figure 17 Inverter Current

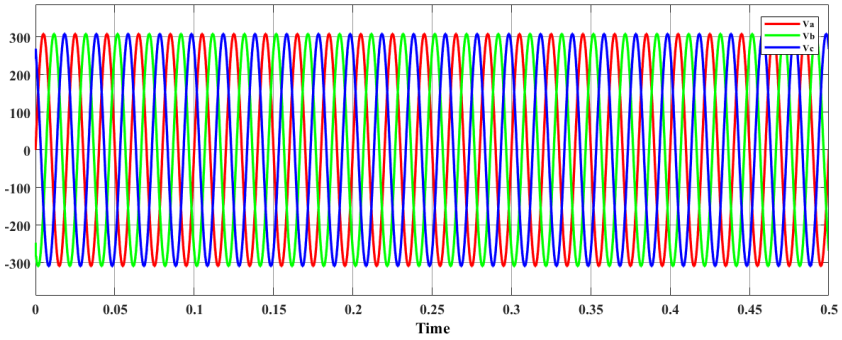

Figure 18 Voltage Grid

5.3 Mixed Method

In the Mixed Method analysis, which combines both V2G and G2V operations, system behavior is evaluated under dynamic bidirectional energy exchange. Vehicle output voltage and current are shown over a 0.5-second time window in Figure 19. Stable AC output is shown by the top subplot, which shows balanced three-phase sinusoidal voltage waveforms (in red, green, and blue), each displaced by 120° and with amplitudes of around ±500V. With large current amplitudes up to ±5000A and three-phase output currents in sinusoidal form, the bottom subplot depicts a high-power electric traction system functioning under controlled circumstances. Battery performance is seen in Figure 20, where the SOC first rises and peaks at 0.2 seconds before falling, signifying a brief charging and discharging process. The battery voltage stays mostly steady with slight variations, indicating a dynamic interaction between the power supply and the EV, but the battery current abruptly declines at 0.4 seconds, most likely as a result of regenerative braking or a load change. The output voltage and current of the vehicle are once again recorded over time in Figure 21. Although slight oscillations suggest switching or load fluctuation, the voltage mostly stays sinusoidal and steady. The output currents exhibit fluctuating amplitudes, going from high-frequency oscillations to a stable state with a lower amplitude for 0.2–0.35 seconds before going back to high-frequency behavior, which might indicate control changes or dynamic mode transitions. Voltage comparisons are shown in Figure 22. The first subplot shows a steady three-phase grid voltage up to small interruptions at 0.2 and 0.4 seconds. In the second subplot, the inverter voltage is stable at first but starts to distort after 0.4 seconds, suggesting that there may be control or load changes. Single-phase voltages from the grid and the inverter are contrasted in the third subplot, which shows early synchronization followed by divergence and instability after interruption. As a sign of system recovery after a disturbance, Figure 23 displays three-phase inverter currents that stay at zero until a rapid stimulation at roughly 0.2 seconds causes transient oscillations that attenuate and stabilize by 0.4 seconds. Figure 24 shows a three-phase voltage waveform with phase voltages Va, Vb, and Vc in red, green, and blue. The waveforms remain consistently sinusoidal, indicating a stable AC supply, except for brief spikes at 0.2 and 0.4 seconds caused by transient events like inverter switching or load changes. The system quickly returns to steady-

state, demonstrating strong resilience and reliability in handling short-term disturbances.

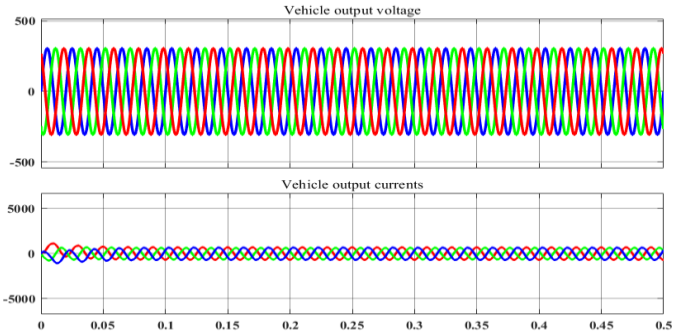

Figure 19. Vehicle output voltage and currents

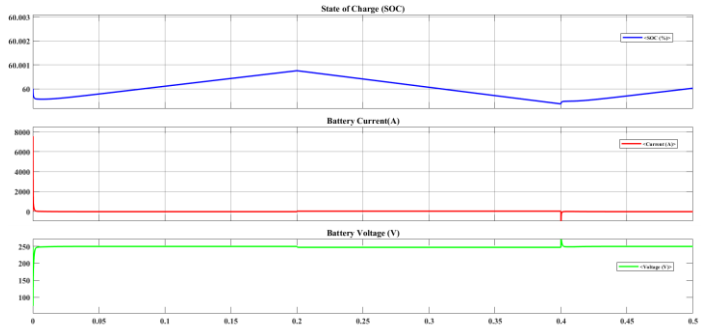

Figure 20 Battery Results

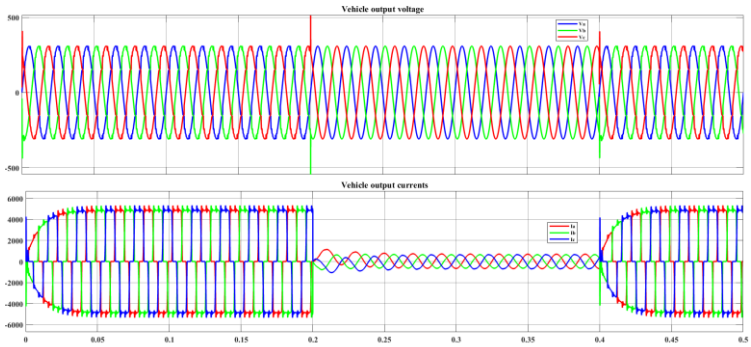

Figure 21 Vehicle Voltage & Current output

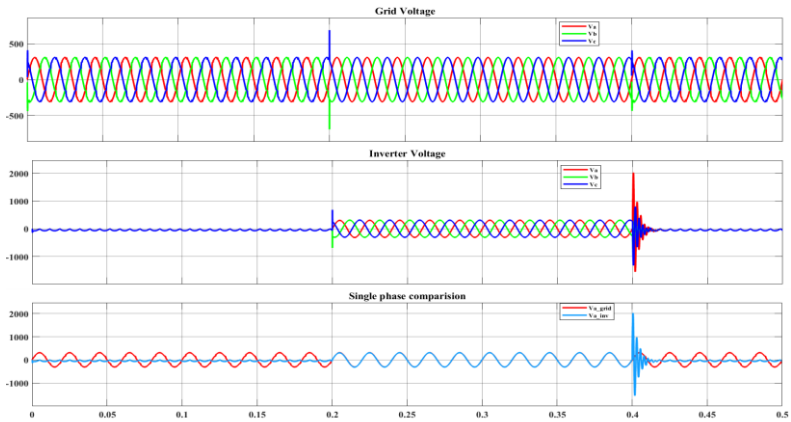

Figure 22 V2G & G2V voltages

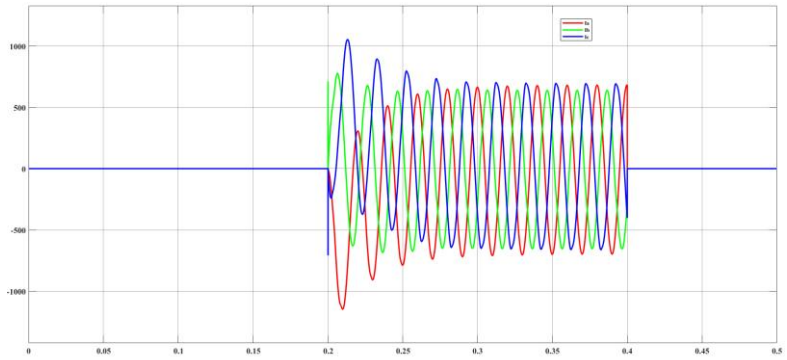

Figure 23 Inverter Currents

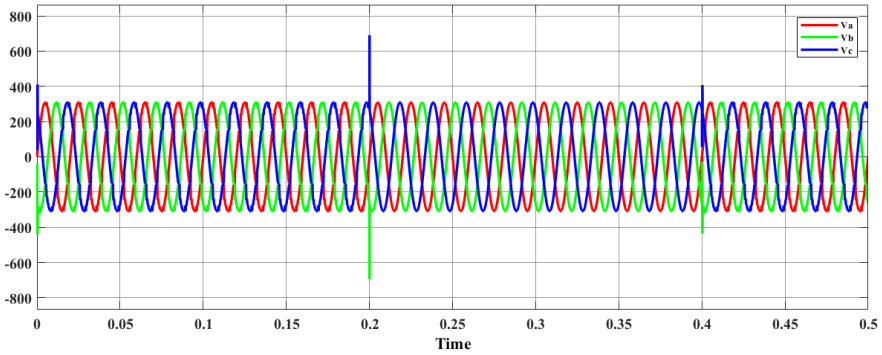

Figure 24 Voltage Grid

5.4 Discussion

The simulation results confirm that the proposed ANFIS-based bidirectional charging system effectively manages energy flow between EVs and the power grid. By combining fuzzy logic with neural network learning, the system dynamically adjusts charging and discharging cycles for optimal power transfer. Compared to traditional PI and rule-based controllers, ANFIS offers faster response, greater adaptability, and reduced transient oscillations, resulting in stable voltage and current waveforms. It enhances grid stability through peak load shaving, frequency control, and reactive power compensation, while also managing battery State of Charge (SOC) to minimize degradation and extend battery life. However, the system's computational complexity remains a challenge for large-scale real-time applications. Future improvements should explore hybrid AI methods and hardware-based validations to boost efficiency and scalability. Despite these challenges, ANFIS-based control shows strong potential for advancing V2G and G2V systems.

6 Conclusion

This research effectively illustrates the efficacy of an ANFIS-based bidirectional battery charging system for V2G and G2V operations. The simulation outcomes verify that the system maintains stable grid voltage, enhances SOC control, and minimizes harmonic distortion, making it exceptionally appropriate for smart grid applications. The ANFIS controller integrates fuzzy logic with neural networks to dynamically regulate power flow, enhancing energy efficiency and prolonging battery life. This approach efficiently aids in peak load control, renewable energy integration, and grid stability, establishing EVs as dynamic energy storage units. Nonetheless, computational complexity persists as a significant constraint, necessitating more optimization and real-time execution for extensive deployment. Future research should concentrate on hybrid AI advancements, hardware validation, and the integration of renewable energy to boost efficiency and scalability. ANFIS-based intelligent control has the potential to transform EV-grid interaction, fostering a more sustainable, dependable, and efficient energy ecology in the future.

References

[1] S. Panchanathan *et al.*, “A Comprehensive Review of the Bidirectional Co€nverter Topologies for the Vehicle-to-Grid System,” *Energies*, vol. 16, no. 5, 2023, doi: 10.3390/en16052503.

[2] M. C. Kisacikoglu, M. Kesler, and L. M.

Tolbert, “Single-phase on-board bidirectional PEV charger for V2G reactive power operation,” *IEEE Trans. Smart Grid*, vol. 6, no. 2, pp. 767–775, 2015, doi: 10.1109/TSG.2014.2360685.

[3] Y. Shanmugam *et al.*, “Solar-powered five-leg inverter-driven quasi-dynamic charging for a slow-moving vehicle,” *Front. Energy Res.*, vol. 11, p. 1115262, 2023.

[4] J. R. Aguero, E. Takayesu, D. Novosel, and R. Masiello, “Modernizing the grid: Challenges and opportunities for a sustainable future,” *IEEE Power Energy Mag.*, vol. 15, no. 3, pp. 74–83, 2017.

[5] G. Buja, M. Bertoluzzo, and C. Fontana, “Reactive power compensation capabilities of V2G-enabled electric vehicles,” *IEEE Trans. power Electron.*, vol. 32, no. 12, pp. 9447–9459, 2017.

[6] O. Elma, U. Cali, and M. Kuzlu, “An overview of bidirectional electric vehicles charging system as a Vehicle to Anything (V2X) under Cyber–Physical Power System (CPPS),” *Energy Reports*, vol. 8, pp. 25–32, 2022.

[7] F. Rippstein, S. Lenk, M. Rudolph, S. Klaiber, and P. Bretschneider, “Flexible artificial intelligence optimization for smart home energy systems with V2X,” in *2022 IEEE Vehicle Power and Propulsion Conference (VPPC)*, IEEE, 2022, pp. 1–6.

[8] D. T. Hoang, P. Wang, D. Niyato, and E. Hossain, “Charging and discharging of plug-in electric vehicles (PEVs) in vehicle-to-grid (V2G) systems: A cyber insurance-based model,” *IEEE Access*, vol. 5, pp. 732–754, 2017.

[9] Z. Fang *et al.*, “Authority allocation strategy for shared steering control considering human-machine mutual trust level,” *IEEE Trans. Intell. Veh.*, vol. 9, no. 1, pp. 2002–2015, 2023.

[10] R. K. Lenka and A. K. Panda, “Grid power quality improvement using a vehicle-to-grid enabled bidirectional off-board electric vehicle battery charger,” *Int. J. Circuit Theory Appl.*, vol. 49, no. 8, pp. 2612–2629, 2021.

[11] F. M. Shakeel and O. P. Malik, “Vehicle-to-grid technology in a micro-grid using DC fast charging architecture,” in *2019 IEEE Canadian Conference of Electrical and Computer Engineering (CCECE)*, IEEE, 2019, pp. 1–4.

[12] P. K. Joseph, E. Devaraj, and A. Gopal, “Overview of wireless charging and vehicle-to-grid integration of electric vehicles using renewable energy for sustainable transportation,” *IET Power Electron.*, vol. 12, no. 4, pp. 627–638, 2019.

[13] G. Sun, Y. Zhang, D. Liao, H. Yu, X. Du, and M. Guizani, “Bus-trajectory-based street-centric routing for message delivery in urban vehicular ad hoc networks,” *IEEE Trans. Veh. Technol.*, vol. 67, no. 8, pp. 7550–7563, 2018.

[14] F. Alfaverh, M. Denaï, and Y. Sun, “Optimal vehicle-to-grid control for supplementary frequency regulation using deep reinforcement learning,” *Electr. Power Syst. Res.*, vol. 214, p. 108949, 2023.

[15] H. Ko, S. Pack, and V. C. M. Leung, “Mobility-aware vehicle-to-grid control algorithm in microgrids,” *IEEE Trans. Intell. Transp. Syst.*, vol. 19, no. 7, pp. 2165–2174, 2018.

[16] Jan Lukas Demuth a and J. Buberger, “Unveiling the power of data in bidirectional charging: A qualitative stakeholder approach exploring the potential and challenges of V2G.” 2024.

[17] M. Amer, J. Masri, U. Sajjad, and K. Hamid, “Electric vehicles: Battery technologies, charging standards, AI communications, challenges, and future directions,” *Energy Convers. Manag. X*, p. 100751, 2024.

[18] U. Sharma and B. Singh, “A bidirectional charging system with the capability to charge electric vehicles with low-voltage powered batteries,” *Electr. Power Syst. Res.*, vol. 243, no. October 2024, p. 111501, 2025, doi: 10.1016/j.epsr.2025.111501.

[19] A. K. P. Rajesh Kumar Lenka, “Grid power quality improvement using a vehicle-to-grid enabled bidirectional off-board electric vehicle battery charger,” 2021, doi: https://doi.org/10.1002/cta.3021.

[20] S. Sagaria, M. van der Kam, and T. Boström, “Conceptualization of a vehicle-to-grid assisted nation-wide renewable energy system–A case study with spain,” *Energy Convers. Manag. X*, vol. 22, p. 100545, 2024.

[21] D. Bogdanov and B. Christian, “Role of smart charging of electric vehicles and vehicle-to-grid in integrated renewables-based energy systems

on country level," 2024, doi: https://doi.org/10.1016/j.energy.2024.131635.

[22] A. Mangipinto, F. Lombardi, F. D. Sanvito, M. Pavičević, S. Quoilin, and E. Colombo, "Impact of mass-scale deployment of electric vehicles and benefits of smart charging across all European countries," *Appl. Energy*, vol. 312, p. 118676, 2022.

[23] S. S. Ravi and M. Aziz, "Utilization of electric vehicles for vehicle-to-grid services: Progress and perspectives," *Energies*, vol. 15, no. 2, p. 589, 2022.

[24] J. Yuan, L. Dorn-Gomba, A. D. Callegaro, J. Reimers, and A. Emadi, "A review of bidirectional on-board chargers for electric vehicles," *IEEE Access*, vol. 9, pp. 51501–51518, 2021, doi: 10.1109/ACCESS.2021.3069448.

[25] O. Turksoy, U. Yilmaz, and A. Teke, "Overview of Battery Charger Topologies in Plug-In Electric and Hybrid Electric Vehicles," *16th Int. Conf. Clean Energy*, no. September, pp. 1–8, 2018.

[26] A. Ali, H. H. H. Mousa, M. F. Shaaban, M. A. Azzouz, and A. S. A. Awad, "A Comprehensive Review on Charging Topologies and Power Electronic Converter Solutions for Electric Vehicles," *J. Mod. Power Syst. Clean Energy*, vol. 12, no. 3, pp. 675–694, 2024, doi: 10.35833/MPCE.2023.000107.

[27] M. S. B. et al. P. K. Maroti, S. Padmanaban, "'The state-of-theart of power electronics converters configurations in electric vehicle technologies,' Power Electronic Devices and Components.," 2022.

[28] and P. B. G. Rituraj, G. R. C Mouli, "'A comprehensive review on off-grid and hybrid charging systems for electric vehicles,'" *IEEE Open J. Ind. Electron. Soc.*, 2022.

[29] J. Pinto, V. Monteiro, H. Goncalves, and J. L. Afonso, "Onboard Reconfigurable Battery Charger for Electric Vehicles With Traction-to-Auxiliary Mode," *Veh. Technol. IEEE Trans.*, vol. 63, pp. 1104–1116, Mar. 2014, doi: 10.1109/TVT.2013.2283531.

[30] U. Sri Anjaneyulu, T. Prathyusha, N. Akhilesh Yadav, V. Prasanth Kumar, and N. Madhava Rao, "A Controllable Bidirectional Battery Charger for Electric Vehicle with Energy Management System," *Int. Res. J. Eng. Technol.*, no. July, 2021.

[31] G. Babu, T. Student, and U. G. C. C. Group-, "Fuzzy logic controller based G2V & V2G Technologies for Three Phase Bi- directional Electric Vehicle Battery Charger," no. 7, pp. 161–169, 2024.

[32] M. Chandra, S. Sahu, M. Vishwanath, P. Kurmi, M. P. Sahu, and A. Professor, "ANFIS-Based Bi-directional Grid Connected EV Charging Station With Battery Storage System," *Int. Res. J. Eng. Technol.*, pp. 27–32, 2024.